Molecular dynamics study of the volumetric and hydrophobic properties of the amphiphilic molecule C_8E_6

A.V. Kim [a,*], N.N. Medvedev [a,b], A. Geiger [c]

[a] Institute of Chemical Kinetics and Combustion SB RAS, Novosibirsk, Russia
[b] Novosibirsk State University, Novosibirsk, Russia
[c] Physical Chemistry, Dortmund University of Technology, Germany

ABSTRACT

A correlation between volumetric properties and hydrophobicity of the surfactant molecule hexaethylene glycol monooctyl ether (C_8E_6) in aqueous solution is studied. Molecular dynamic models of a single C_8E_6 molecule surrounded by 7075 water molecules were simulated and analyzed for different temperatures at ambient pressure. The apparent volume (V_{app}) of the solute molecule was calculated. The intrinsic volume of the solute molecule (V_{int}) was defined as the volume of the Voronoi region of the solute molecule (calculated on the basis of power (radical) Voronoi tessellation). It is shown that the contribution of the hydration water to the apparent volume ($\Delta V = V_{app} - V_{int}$) is negative for lower temperatures and becomes positive for higher temperatures. The degree of hydrophobicity of C_8E_6 was also calculated by two different methods. It was shown that the solute molecule is hydrophilic at lower temperatures and becomes hydrophobic with temperature increase. This change occurs at a temperature which coincides well with the temperature, where the volumetric characteristic ΔV changes its sign.

1. Introduction

Alcohol ethoxylates are a basic class of nonionic surfactants, which are widely used as emulsifiers in food, pharmaceuticals, and cosmetics; in detergents, household and industrial cleaners; in agriculture, textile, paper, oil and other industries. All such molecules are amphiphilic, tending to dissolve in both aqueous and oil phases and reduce the surface tension of liquids. If the molecule consists of a hydrophobic linear alkyl chain with n C-atoms, a hydrophilic tail of m ethylene-oxide units, and a terminating hydroxyl group, it is abbreviated as C_nE_m [1], Fig. 1. We study here a hexaethylene glycol monooctyl ether (C_8E_6) molecule in water. Aqueous solutions of this surfactant exhibit a lower critical solution temperature (LCST) and change its transparency with heating. This transition temperature, being referred to as cloud point, is close to 348 K [2]. This transition is a consequence of the fact that C_8E_6 molecules become more hydrophobic with temperature increase and thus show an increased tendency for mutual aggregation.

The hydrophobic properties of molecules of the C_nE_m family were studied in [2] by molecular dynamics simulations. The degree of hydrophobicity was characterized there by the strength of interaction with a hydrophobic test particle, quantified by the difference between the free energy of a neon atom in the vicinity of the solute and in bulk water. The calculation of free energies was performed by the Widom test particle insertion method [3,4]. It was shown that the free energy difference changes its sign at a temperature, which corresponds to the experimental cloud point of the solution [2].

Hydrophobic particles tend to aggregate spontaneously in water, driven by the so called *hydrophobic interaction* [5]. As implied above for the special case of interaction with a neon atom, a measure of hydrophobicity is the free energy of the *hydrophobic interaction* between the solute molecules. If this energy is negative, aggregation occurs [5]. Hydrophobic interaction manifests itself in numerous phenomena [6], including the processes of self-assembling, formation of micelles and bilayers and protein folding. The free energy of hydrophobic interaction is a component of the total solvation free energy for two or more solute molecules in water. For the calculation of this component one can use thermodynamic cycles, connecting the states of solutes in solution and in vacuum [7,8]. Solvation free energies can be calculated with the help of multistate Bennett acceptance ratio method (MBAR) [9,4,10].

Another important characteristic of a solution is the *partial molar volume* (PMV) of its components. For infinitely diluted solutes its PMV correspond to the so-called *apparent volume* (V_{app}) of the solute [11]. The term is usually used when working with computer models of solutions with a single solute molecule in the model box. According to the well-known legend, Archimedes found the volume of the golden crown, assuming it is equal to the volume of the

H-(CH$_2$)$_8$-(O-CH$_2$- CH$_2$)$_6$-OH

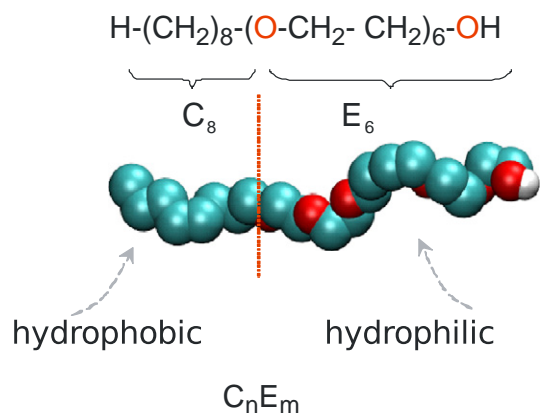C$_8$ E$_6$

hydrophobic   hydrophilic

C$_n$E$_m$

Fig. 1. Amphiphilic molecule C$_8$E$_6$.

displaced water. But for a molecule the observed increase in the solution volume has contributions from both the solute molecule and the changing of the solvent structure around the solute. Thereby, the observed apparent volume can be written as [12–15]:

$$V_{app} = V_{int} + \Delta V. \tag{1}$$

Each of the two contributions can be further decomposed into separate contributions. The *intrinsic* volume V_{int} includes the van der Waals volume of the solute molecule, internal voids and a part of the empty space from the boundary region between solute and solvent. The contribution ΔV originates from the density change of the solvent. It is considered as the difference between the solvent volume in the solution, being influenced by the presence of the solute, and the volume of the same amount of the pure solvent. One can try to extract different components for ΔV [16–19]. However, in this paper we deal with the division of the apparent volume into two main components, according to formula (1).

In this paper we study the volumetric and thermodynamic properties of a C$_8$E$_6$ molecule in aqueous solution at different temperatures. We calculate the contribution ΔV of the water to the apparent volume of the solute molecule and its hydrophobicity to investigate the behavior of these characteristics with temperature.

2. Methods

2.1. MD details

A set of molecular dynamic models of aqueous solutions of C$_8$E$_6$ molecule was generated for different temperatures in the interval from 250 to 400 K in 10 degree increment at ambient pressure. Each model contains one molecule of C$_8$E$_6$ and 7075 water molecules. Such a relatively large amount of water guarantees the absence of interaction of the solute molecule with its periodic images. The simulation was performed using GROMACS package [20]. Methyl and ethylene groups were represented by united atoms with the force-field proposed in [21,22]. For water–water interactions we used TIP4P-Ew model [23]. The solute–solvent interaction was calculated according Lorentz–Berthelot mixing rules.

One nanosecond relaxation period with Berendsen barostat and V-rescaling thermostat was followed by a productive run of 20 ns. Parrinello–Rahman pressure coupling [24] and Nose–Hoover temperature coupling [25] were used for the production runs. The values of the time constants for pressure and temperature coupling were of 1.0 ps and 0.5 ps respectively. Fast particle mesh Ewald summation was applied for electrostatic interaction [26] with a real space cutoff of 1.2 nm and a grid spacing of 0.12 nm and fourth-order interpolation.

Van der Waals interactions were cutoff at 1.2 nm with long range dispersion corrections for energy and pressure. Integration step of 2 fs was used, and the configurations were sampled every 10 ps for the further processing.

2.2. Apparent volume calculation

From the point of view of an experimenter the apparent volume is defined as the difference between the volume of the solution and the volume of the corresponding amount of pure solvent. In the case of molecular dynamics simulation the apparent volume can be found as the difference between the mean volume of the model box containing the solution and containing the pure solvent:

$$V_{app} = <V_{box}^{Solution}> - <V_{box}^{Solvent}>. \tag{2}$$

Both systems should be generated at the same pressure and temperature, and the number of water molecules in pure solvent should be the same as in the solution.

However, in some cases this *direct* method gives insufficient accuracy, see [19] and references therein. The value V_{app} in formula (2) is the difference of two relatively large quantities, each of them being calculated with an error. The error can be small, around 0.1%, and it can be neglected in many cases. However, as the apparent volume represents usually a small part of the model box volume, its error may become quite high. Indeed, if it is one-hundredth of the model box volume ($V_{app} \sim 10^{-2} V_{box}^{Solvent}$), it is easy to estimate, that the 0.1% inaccuracy of the mean value of the model box volume leads to 10% inaccuracy in the apparent volume [19].

There is another way to calculate the apparent volume, supposing that the solute perturbs the surrounding water only in the vicinity. It is assumed that biomolecules affect not more than two or three molecular layers, and at larger distances the water structure is not perturbed. So it is proposed to use the formula:

$$V_{app}(R) = V(R) - N(R)/\rho_0 + k\beta_T T, \tag{3}$$

where $V(R)$ means a volume around the solute, including both the solute and its hydration shell, the parameter R characterizes the scale of this region. $N(R)$ means the number of the solvent molecules, whose centers are inside the selected volume $V(R)$, ρ_0 is the density of pure water at the same temperature and pressure. The term $k\beta_T T$ is necessary, as the volume $V(R)$ and the number $N(R)$ are always considered around the solute molecule without taking into account translational degrees of freedom of the solute molecule (i.e. without motion of the solute in the solution), see for example [27,28], β_T is the isothermal compressibility of water. However, this contribution is small and changes slightly in the desired temperature interval, so it is usually ignored.

Note that the region $V(R)$ in formula (3) can be rather arbitrary. It does not matter where and how to draw its border, as long as it lies entirely in bulk water.

In the case of spherical solute molecules formula (3) can be reduced to the well-known Kirkwood–Buff formula for the calculation of the partial molar volume [29,30]:

$$V_{app} = -G + k\beta_T T, \tag{4}$$

where G is the Kirkwood–Buff integral:

$$G = 4\pi \int \left(\frac{\rho(r)}{\rho_0} - 1 \right) r^2 dr, \tag{5}$$

$\rho(r)$ is the radial distribution function of the water density around the solute, and ρ_0 is its asymptotic value, that is for pure water. The volume $V(R)$ in Eq. (3) is obtained from the integration of the second

term in integrand (5), and $N(R)/\rho_0$ is obviously from the first term in Eq. (5). Recall that the function $G(R)$ is a decaying oscillating function. The Kirkwood–Buff approach is commonly used in conjunction with RISM theory, where the function $\rho(r)$ is calculated theoretically. Thereafter it is not difficult to calculate the integral (5) [31–33]. However, when working with computer models, where all coordinates of atoms are known, we can use the general formula (3), especially if the solute has a complex shape.

Usually the distance R to the polyatomic molecule is measured up to the surface of the closest atom. In molecular biology there is a well-known SAS (solvent accessible surface), which lies at a distance equal to the radius of a water molecule (1.4A) [34–36]. But in our case the distance R can be arbitrary and rather large. The volume $V(R)$ in formula (3) can be calculated as the volume inside such an R-surface, Fig. 2.

However this calculation is not easy in general. It reduces to the problem of finding the volume of a union of spheres of different radii: the spheres are centered on the solute atoms and have radii equal to $R + R_a$, where R_a is the radius of the corresponding atom. Note, at $R = 0$ we get the van der Waals volume of the solute molecule (volume of the union of atoms of molecule). Methods for the calculation of such volumes $V(R)$ were discussed in [37,38].

The calculation of $N(R)$ for complex solute molecules does not cause any difficulty. As in the case of a spherical solute molecule, it is enough to choose those water molecules, whose centers are within the given distance R.

The dashed line in Fig. 3 shows the behavior of the apparent volume $V_{app}(R)$ of C_8E_6 molecule calculated by the discussed method (we call it *traditional* method [15]). The required value is defined by the asymptote of this function. The oscillations which are continuing up to 1 nm are the manifestation of the oscillations of the water density $\rho(R)$ around the solute molecule.

These oscillations can lead to errors in estimating the asymptotic value of V_{app}. It requires the calculation of the $V_{app}(R)$ profile up to a fairly large distance R. With an increase of R, the problem of accuracy of the water density ρ_0, which was discussed above for the *direct* method, arises again. In this case the volume of $V(R)$ becomes very large in comparison with the volume of the solute molecule.

It is possible to avoid this problem, if we use another method, called *combined* [15]. The only difference of this approach from the traditional one is the calculation of $V(R)$ with the help of Voronoi cells. Instead of calculating the volume inside the R-surface, we simply sum the Voronoi cell volumes of all atoms with centers inside the R-surface, Fig. 4. This comprises all atoms of the solute molecule and $N(R)$ water molecules. On this way we avoid the difficult task of the traditional method (to calculate the volume inside a complex surface), but now we should be able to calculate the Voronoi cells.
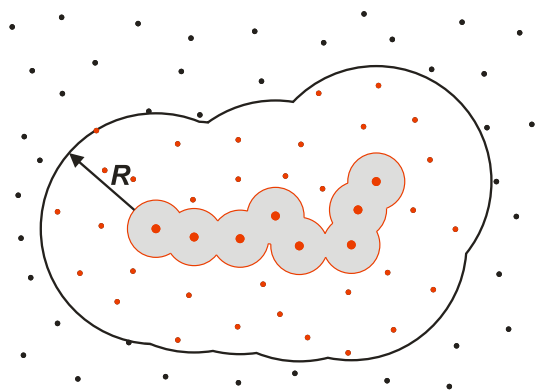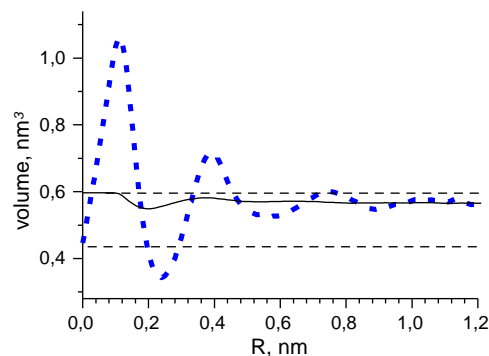

Fig. 3. Profile of the apparent volume of the C_8E_6 molecule in aqueous solution, calculated according to formula (3) by the *traditional* (dashed line) and the *combined* methods (solid line). Horizontal dashed lines show the van der Waals volume of the molecule (lower line), and the Voronoi volume of the molecule, intrinsic volume (upper line).

However, there are efficient programs for such calculations in geometry libraries and packages.

The profile $V_{app}(R)$ calculated by the combined method is also shown in Fig. 3 (solid line). In this case there are no large oscillations as for the traditional method. This is because the solvent molecules in formula (3) are now taken into account with their volumes. Incrementing R by a value ΔR in the traditional method results in a monotonic increase in volume as $4\pi R^2 \Delta R$, independent of how many new molecules appear in the volume. However, the number $N(R)$ changes according to the current value of the $\rho(R)$ function. In the combined method the increase of R results in the synchronous change of the first and second terms in the right part of formula (3). Thus the oscillations of $\rho(R)$ do not appear.

Both methods give the same asymptote for $V_{app}(R)$, Fig. 3. However now it is achieved at significantly smaller distances, therefore with smaller errors. The basic calculations of the apparent volumes in this paper were performed with the combined method.

2.3. Components of the apparent volume

We propose that the intrinsic volume V_{int} of a solute molecule is the Voronoi volume of this molecule in solution [39–42,15]. This is the region of space, all points in which are closer to the solute molecule than to any solvent molecule. The Voronoi region can be defined for an arbitrary complex solute, Fig. 5.

Thus the intrinsic volume of the solute molecule includes the van-der Waals volume, the empty space volume inside the molecule

Fig. 2. $V(R)$ region around the solute molecule. The surface of the region is spaced at the distance R from the molecule. The solute molecule is shown by gray disks, the separate dots mean the centers of solvent molecules.
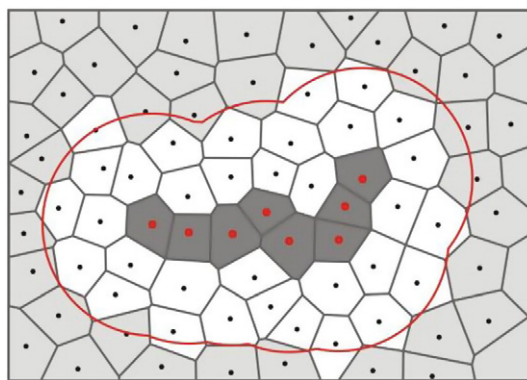

Fig. 4. $V(R)$ volume by the *combined* method. The surface of the region is located at a distance R from the solute molecule as in Fig. 2. The volume is defined as the sum of the Voronoi cell volumes of atoms of the solute molecule and water molecules inside the surface: including the solute molecule Voronoi volume (dark) and solvent molecules (white).
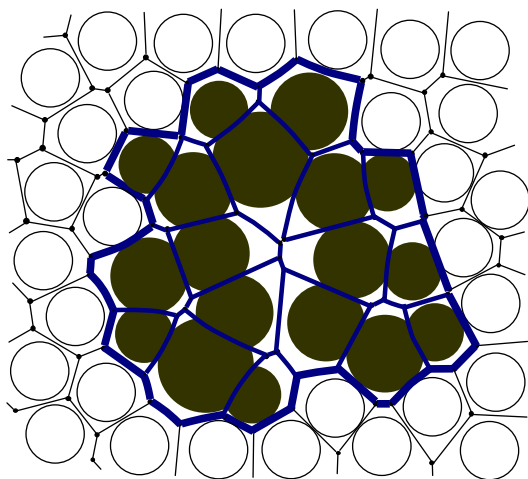
Fig. 5. Voronoi region of a polyatomic solute molecule. It is the sum of Voronoi regions of all its atoms. The solute molecule is represented by black disks, the solvent by empty disks. The border of the solute Voronoi region is shown by a thick line. Voronoi S-tessellation is used for the decomposition of the solution in this figure.

and that part of the volume outside, which is closer to the solute than to the solvent.

In recall, there are different types of the Voronoi tessellations. They differ in how the distance to the atom is measured. Three types are of interest to physical applications. The first one is the *classical*, where only atomic centers are considered. The next two tessellations take into account atomic radii. It is the additively-weighted (*S-tessellation*) and the *power* (or radical) tessellation, see for example [15] and references therein. For the calculation of the apparent volume it does not matter which type of tessellation is used. However for the calculation of the Voronoi region, the type of tessellation plays a role. In this paper the power tessellation is used. The values of the atomic Lennard–Jones σ parameters of the molecular dynamics force field were used as the corresponding atomic radii.

Thus, if the apparent volume V_{app} and the intrinsic volume V_{int} were calculated as it was described above, the contribution of the solvent ΔV can be easily found from formula (1): $\Delta V = V_{app} - V_{int}$.

2.4. Hydrophobicity

Following the papers [2,43,44] we calculated the excess chemical potential of a neon atom ($\sigma = 3{,}035$ Å, $\varepsilon/k_B = 18{,}6$ K [45]) in a solution of a C_8E_6 molecule and in pure water. The calculation was performed, using the Widom test particle insertion method [3,4]. The excess chemical potential of a test particle is calculated in the NPT ensemble according to:

$$\mu_{ex} = -kT \ln\left(\left\langle V \int e^{-\Delta U/kT} ds \right\rangle / \langle V \rangle\right), \qquad (6)$$

where ΔU is the potential energy of the inserted particle, integration is performed over the model box, V is the volume of the box. The brackets $< \ldots >$ indicate averaging over all sampled configurations of the isothermal-isobaric MD-trajectory.

The difference $\Delta\mu$ of the chemical potential values of neon in solution and in bulk water can be a measure for the estimation of the hydrophobicity of C_8E_6 molecule:

$$\Delta\mu = \mu_{ex}^{Solution} - \mu_{ex}^{Water}. \qquad (7)$$

If the chemical potential of neon in solution is less than in bulk water, it means the C_8E_6 molecule facilitates the neon solvation and can be considered as hydrophobic (akin to neon). If the C_8E_6 molecule

does not help the neon to solvate ($\Delta\mu > 0$) then it can be considered as hydrophilic. The GROMACS implementation of the Widom method was used for our calculations [20,18].

Note, $\Delta\mu$ contains a contribution from the direct interaction between neon and the C_8E_6 molecule and from the interaction between these molecules mediated by water. The last contribution means the hydrophobic interaction. The first contribution can be estimated easily by the Widom method, when water is removed (decoupled) from the solution. We found this value is about 10% of the total contribution calculated by formula (7). Thus the value $\Delta\mu$ can be used for the estimation of the hydrophobicity of the C_8E_6 molecule.

We also calculated the hydrophobic interaction between C_8E_6 molecules. The *multistate Bennett acceptance ratio*, or *MBAR method* [46,9] which combines the weighted histogram analysis (WHAM) [47] and the BAR method [10,4] implemented in GROMACS 4.5 was used. In this approach a set of close intermediate states between a given initial and final state are simulated. The free energy differences are calculated for the neighboring states and added up on the path from the initial to the final state. At the decoupling of the interaction between the molecules the charges were turned off first, and then the Lennard–Jones terms [9]. A linear approach for the change of the potential energy parameters was used. The soft core approach for decoupling of the van der Waals interactions was applied as in [48]. A dual topology was used for constructing the pathway between initial and final states of molecules. For each pathway, connecting initial and final states, 21 intermediate states were simulated, each of 1 ns. In some cases the number of intermediate states was increased up to 50, to reduce the statistical uncertainty of the free energy difference between neighboring states.

The hydrophobic interaction implies the presence of more than one solute molecule in solution. We used 27 C_8E_6 molecules in an environment of 6417 water molecules, this corresponds to a concentration of 8.43% wt. The scheme of the thermodynamic cycle used for the calculation of hydrophobic interaction free energy is shown in Fig. 6.

State I is made up of 27 non-interacting C_8E_6 molecules and pure water. In molecular dynamics simulation this corresponds to a "solution" where all intermolecular interactions of C_8E_6 molecules with each other and with water are turned off. State II is the real solution: all 27 solute molecules interact with each other and with water. Besides the direct interaction between the solute molecules there should be present an additional interaction, which is mediated by water. This is the hydrophobic interaction. The value ΔG between states I and II was calculated by the MBAR method. It is presented in Fig. 7 as function of temperature by squares. Negative values of ΔG indicate that our solute molecules prefer to be dissolved in water. However, the decrease of the absolute value of ΔG with temperature points out that the dissolution becomes less profitable with heating. State III differs from state I in that the interaction between the solute molecules is turned on. The free energy difference between these states ΔG_{mm} was also calculated, gradually turning on the interaction between the 27 molecules without interaction with water. The difference ($\Delta G - \Delta G_{mm}$) is shown in Fig. 7 with triangles. On the path from states III to II, the interaction between the solute molecules and water was turned on. The free energy difference between these states can be presented as a sum of two contributions: ΔG_{mw} due to direct interaction of the solute with water, and the desired hydrophobic interaction ΔG_h.

According to the thermodynamic cycle Fig. 6 (a) we can write the relation:

$$\Delta G = \Delta G_{mw} + \Delta G_{mm} + \Delta G_h. \qquad (8)$$

Thus, to determine the value of hydrophobic interaction ΔG_h we need to know ΔG_{mw}. The direct interaction of the solute with water can be calculated by dissolving one solute molecule in water, Fig. 6 (b). We calculated the free energy ΔG^1_{mw} of such a transition
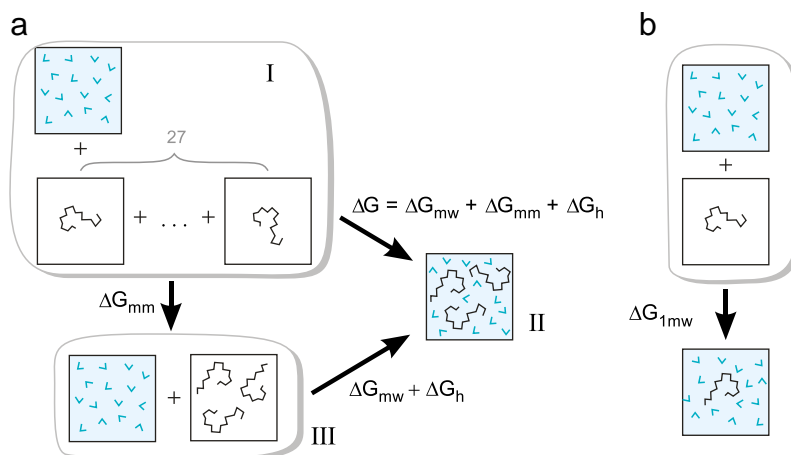
Fig. 6. a) A thermodynamic cycle for the calculation of the free energy of hydrophobic interaction. ΔG is the free energy for the transition of 27 non-interacting solute molecules (I) into water solution (II). ΔG_{mm} is the free energy of turning on the interaction between 27 C_8E_6 molecules in vacuum (I), (III). $\Delta G_{mw} + \Delta G_h$ is the free energy for the transition of 27 interacting solute molecules (III) into solution (II). b) A path for the calculation of the free energy for dissolving one C_8E_6 molecule: ΔG^1_{mw}.

by turning on the interaction of one C_8E_6 molecule with water. The required value for 27 solute molecules can be estimated as $\Delta G_{mw} = 27 * \Delta G^1_{mw}$. The temperature behavior of this value is shown in Fig. 7 with diamonds. Thus the required free energy of hydrophobic interaction at the given concentration can be obtained as difference between this curve and the $(\Delta G - \Delta G_{mm})$ curve, Fig. 7.

Thus the free energy of hydrophobic interaction in the system with 27 molecules we can find from the relation:

$$\Delta G = 27\Delta G_{1mw} + \Delta G_{mm} + \Delta G_h. \tag{9}$$

3. Results

Fig. 8 shows the temperature behavior of the apparent volume of the C_8E_6 molecule and its components V_{int} and ΔV, calculated as it was described above.

For the amphiphilic C_8E_6 molecule both the apparent and intrinsic volumes rise with temperature, but their rates are different. This
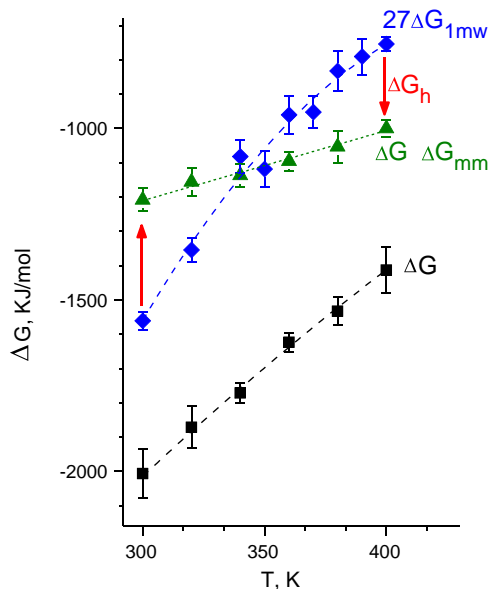
results in a change of the ΔV sign. At lower temperatures the apparent volume V_{app} is less than the intrinsic one, thus ΔV is negative. This means, that the water density around the C_8E_6 molecule is higher than in the bulk. When heated, the apparent volume is larger than the intrinsic thus ΔV becomes positive. This corresponds to a less dense, more open structure of hydration water, which is typical for hydrophobic molecules.

We also calculated the partial contributions from the hydrophilic and hydrophobic parts of the C_8E_6 molecule to ΔV, Fig. 10. The water molecules were assigned to the hydrophilic part if they are positioned closer to the atoms of this part of the molecule than to the atoms of the hydrophobic part, and vice versa, Fig. 9.

As one can see from Fig. 10, the contribution ΔV from the hydrophilic side of the solute molecule is negative up to very high temperatures and lower than the contribution from the hydrophobic one for all temperatures. This is consistent with the well-accepted concept, that the hydration water near hydrophilic groups is denser than bulk water, whereas the water in the hydrophobic shell has a more open structure. This is due to the fact that attractive electrostatic and hydrogen bond interactions between solute and solvent lead to the constriction of the hydrophilic hydration shell, whereas the
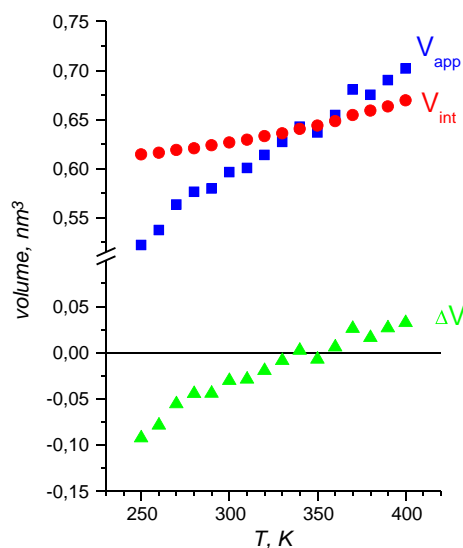

Fig. 7. The temperature behavior of the free energy components calculated for the thermodynamic cycle shown in Fig. 6.

Fig. 8. The temperature behavior of the apparent volume V_{app} of C_8E_6 molecule and it components: intrinsic V_{int} volume and the contribution of water ΔV.
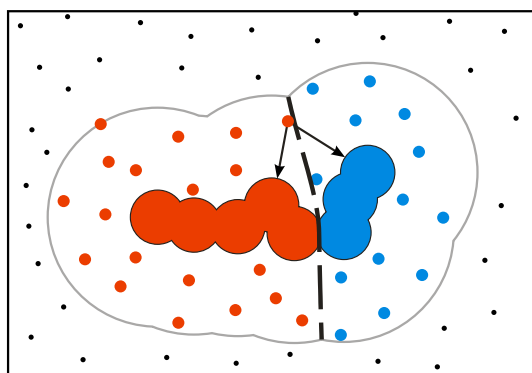
Fig. 9. Illustration of the water molecules assigned to the hydrophilic (left) and hydrophobic (right) parts of an amphiphilic molecule.

Fig. 11. The difference of the chemical potentials of neon in C_8E_6 solution and in bulk water.

interaction of a hydrophobic solute with water is weak and the dominating interaction is the hydrogen bonding between the hydration water molecules, which leads to the formation of a loosely packed environment. Contrary to this opposing behavior, the temperature dependence of ΔV is similar both for hydrophilic and hydrophobic parts: both show a positive slope. This can be understood on the basis of our recent paper [18], where it was shown that the main contribution to the thermal expansion of a polypeptide molecule in water is caused by the boundary area between the solute molecule and the solvent (the so called "thermal volume"). It was shown that the boundary area expands faster than bulk water, because of less hydrogen-bonds across the boundary area, both in the hydrophilic and the hydrophobic shell. If ΔV is normalized by the corresponding number of the atomic units (6 ethylene-oxide and 8 methylene groups) the contribution per hydrophobic group increases faster, than for the hydrophilic one, see insert in Fig. 10. This is in line with the just discussed fact, that there are more hydrogen bonds around the hydrophilic part than between the hydrophobic group. Thus the density of the hydration water changes more slowly in the hydrophilic, compared with the hydrophobic part.

The difference of the chemical potential of neon in solution and in the bulk $\Delta\mu$ calculated according to formula (7), is shown in Fig. 11 as a function of temperature.

The decrease of the value of $\Delta\mu$ with temperature indicates the tendency of neon to aggregate with the C_8E_6 molecule. Note, the value of $\Delta\mu$ changes the sign at about 340 K, which is close to the temperature, where ΔV changes its sign, see Fig. 8 (~350 K), and it is close to the experimental cloud point of C_8E_6 (348 K) [2].

The free energy of hydrophobic interaction between C_8E_6 molecules, calculated according to formula (9) is shown in Fig. 12. There are two
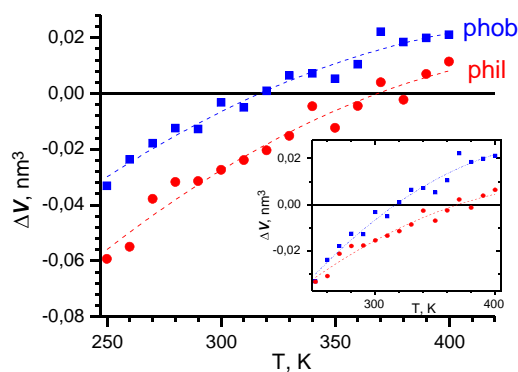
sets of the data points in this figure. One of them (the upper three points) results from sampling problems which arose in our calculation in the process of decoupling of the Lennard–Jones interactions between C_8E_6 molecules, as described above. The solute molecules being almost decoupled stuck together, and the system remained trapped in this state for a very long period of time. Such trapped configurations give a higher value of the free energy for the hydrophobic interaction. However, the trapping was absent in the main part of simulation (from these, the lower data points have been derived).

We ignored the results with the trapping and use the lower curve in Fig. 12. The value ΔG_h is positive at the low temperatures, that means the C_8E_6 molecules are hydrophilic (they show a preference to be surrounded by water molecules). With increasing temperature ΔG_h becomes negative. This means the solute molecules are prone to aggregate. The temperature of the sign change is about 345 K, again close to the transition temperature of the volumetric characteristic ΔV and nearly coinciding with the experimental cloud point.

4. Summary

In this paper we calculated both volumetric and free energy characteristics for the amphiphilic molecule C_8E_6 in aqueous solution at different temperatures. A comparable behavior of these properties with increasing temperature was obtained.

The apparent volume of the dissolved molecule (that is the partial molar volume of the solute at infinite dilution) and its components (the intrinsic volume of the solute molecule and the contribution of the solvent to the apparent volume) were calculated. The apparent volume can be calculated by different methods. One of them (the traditional) is similar to the Kirkwood–Buff approach. The second one is a combined method, where the volume around the molecule is

Fig. 10. The partial contributions of water to the apparent volume of the C_8E_6 molecule, originating from the hydrophobic (squares) and hydrophilic (circles) parts. Insert: same data, but normalized by the number of the molecular units (8 methylene and 6 ethylene-oxide atomic groups).
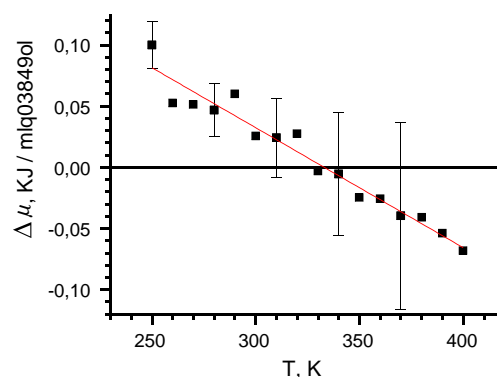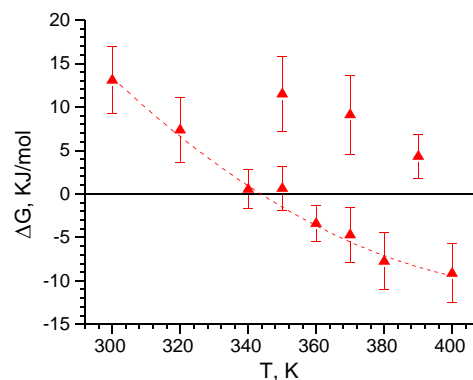

Fig. 12. Calculation free energy of the hydrophobic interaction for C_8E_6 molecule in water solution by formula (9).

calculated with the help of a Voronoi technique. It was shown that the combined method is more preferable than the traditional one. The intrinsic volume of the solute molecule was defined as the volume of the Voronoi region of the molecule in solution, being calculated by using the power Voronoi tessellation. The solvent contribution ΔV was calculated as the difference between the apparent and the intrinsic volume. It is shown that the value of ΔV increases with temperature and changes its sign from negative to positive. It correlates with the behavior of the degree of hydrophobicity of the C_8E_6 molecule. We used two different measures for the hydrophobicity: first we calculated it as the difference of the chemical potentials of a neon atom in pure water and in a solution with a single C_8E_6 molecule. The other technique is based on the MBAR method for the calculation of the free energy of interaction between the solute molecules in water. Both methods demonstrate that the hydrophobicity of a molecule is a question of temperature: the C_8E_6 molecule is hydrophilic at lower temperatures and becomes hydrophobic with increasing temperature. The transition temperature is qualitatively the same as for the change of sign for ΔV.

Thus the behavior of a volumetric characteristic reflects the hydrophobic property of the amphiphilic molecule C_8E_6. Since the volumetric properties can be calculated more easily in comparison with free energy calculations, the results obtained in this paper suggests that the solvent contribution to the apparent volume ΔV can be used as a measure for the hydrophobicity of a molecule.

Acknowledgments

References

[1] T.F. Tadros, Applied surfactants: principles and applications, Wiley-VCH Verlag GmbH & Co. KGaA, Weinheim, 2005.
[2] D. Paschek, T. Engels, A. Geiger, W. von Rybinski, Colloids and Surfaces A: Physicochemical and Engineering Aspects 156 (1999) 489–500.
[3] B. Widom, Journal of Chemical Physics 39 (1963) 2808.
[4] D. Frenkel, B. Smit, Understanding molecular simulation, From Algorithms to Applications, Academic Press, USA, San Diego, 1996.
[5] D. Chandler, Nature 437 (2005) 640–647, http://dx.doi.org/10.1038/nature04162.
[6] E. Meyer, K.J. Rosenberg, J. Israelachvili, Proceedings of the National Academy of Sciences of the United States of America 103 (43) (2006) 15739–15746.
[7] A. Villa, A.E. Mark, Journal of Computational Chemistry 23 (5) (2002) 548–553.
[8] D.L. Mobley, J.D. Chodera, K.A. Dill, Journal of Chemical Theory and Computation 3 (4) (2007) 1231–1235.
[9] M.R. Shirts, D.L. Mobley, Biomolecular Simulations Methods in Molecular Biology 924 (2013) 271–311.
[10] C.H. Bennett, Journal of Computational Physics 22 (1976) 245–268.
[11] E.A. Melwyn-Hughes, Physical Chemistry, Pergamon Press, London, 1961.
[12] L. Mitra, N. Smolin, R. Ravindra, C. Royer, R. Winter, Physical Chemistry Chemical Physics 8 (2006) 1249–1265.
[13] I. Brovchenko, R.R. Burri, A. Krukau, A. Oleinikova, R. Winter, Journal of Chemical Physics 129 (2008) 195101.
[14] I. Brovchenko, R.R. Burri, A. Krukau, A. Oleinikova, R. Winter, Journal of Chemical Physics 129 (2008) 195101.
[15] V.P. Voloshin, N.N. Medvedev, M.N. Andrews, R.R. Burri, R. Winter, A. Geiger, Journal of Physical Chemistry B 115 (48) (2011) 14217–14228.
[16] T.V. Chalikian, Annual Review of Biophysics and Biomolecular Structure 32 (2003) 207–235.
[17] T. Imai, Condensed Matter Physics 10 3 (51) (2007) 343–361.
[18] A.V. Kim, V.P. Voloshin, N.N. Medvedev, A. Geiger, Transactions on Computational Science Journal, Springer (2013), (in press).
[19] N.N. Medvedev, V.P. Voloshin, A.V. Kim, A.V. Anikeenko, A. Geiger, Journal of Structural Chemistry (Zhurnal Strukturnoi Khimii), (2013), (in press).
[20] B. Hess, C. Kutzner, D. van der Spoel, E. Lindahl, Journal of Chemical Theory and Computation 4 (3) (2008) 435–447.
[21] J.M. Stubbs, J.J. Potoff, J.I. Siepmann, Journal of Chemical Physics B 108 (45) (2004) 17596–17605, http://dx.doi.org/10.1021/jp049459w.
[22] J. Fischer, D. Paschek, A. Geiger, G. Sadowski, Journal of Physical Chemistry B 112 (8) (2008) 2388–2398.
[23] H.W. Horn, W.C. Swope, J.W. Pitera, Journal of Chemical Physics 120 (20) (2004) 9665–9678.
[24] M. Parrinello, A. Rahman, Journal of Applied Physics 52 (1981) 1782–1790.
[25] W.G. Hoover, Physical Review A 31 (1985) 1695–1697.
[26] U. Essmann, L. Perera, M.L. Berkowitz, T.A. Darden, H. Lee, L.G. Pedersen, Journal of Chemical Physics 103 (1995) 8577–8593.
[27] N. Matubayas, R.M. Levy, Journal of Physical Chemistry 100 (1996) 2681–2688.
[28] M.S. Moghaddam, Hue Sun Chan, Journal of Chemical Physics 126 (2007) 114507.
[29] J.G. Kirkwood, F.P. Buff, Journal of Chemical Physics 19 (1951) 774.
[30] A. Ben-Naim, Molecular Theory of Solutions, Oxford University Press, Oxford, 2006.
[31] A. Ben-Naim, Journal of Chemical Physics 128 (2008) 234501.
[32] N. Patel, D.N. Dubins, R. Pomes, T.V. Chalikian, Biophysical Chemistry 161 (2012) 46–49.
[33] I. Yu, T. Tasaki, K. Nakada, M. Nagaoka, Journal of Physical Chemistry B 114 (2010) 12392–12397.
[34] F.M. Richards, Methods in Enzymology, 115, 1985, pp. 440–464.
[35] J. Liang, Biological and Medical Physics, Biomedical Engineering, Springer, New York, 2007, pp. 181–206.
[36] M.L. Connolly, Journal of the American Chemical Society 107 (1985) 1118–1124.
[37] V.P. Voloshin, A.V. Anikeenko, N.N. Medvedev, A. Geiger, Proceedings of Eighth International Symposium on Voronoi Diagrams in Science and Engineering (ISVD 2011), Qingdao, China, 2011, pp. 170–176.
[38] F. Cazals, H. Kanhere, S. Loriot, Computing the Volume of a Union of Balls a Certified Algorithm, Sophia Antipolis Cedex, France, 2009.
[39] P. Procacci, R. Scateni, International Journal of Quantum Chemistry 42 (1992) 1515–1528.
[40] E. Paci, M. Marchi, Proceedings of the National Academy of Sciences of the United States of America 93 (1996) 11609–11614.
[41] V. Lounnas, B.M. Pettitt, Proteins: Structure, Function, and Genetics 18 (1994) 133–147.
[42] M. Marchi, Journal of Physical Chemistry B 107 (2003) 6598–6602.
[43] D. Paschek, Journal of Chemical Physics 120 (22) (2004) 10605–10617, http://dx.doi.org/10.1063/1.1737294.
[44] D. Paschek, R. Ludwig, J. Holzmann, in: E. Wilhelm, T.M. Letcher (Eds.), Heat Capacities: Liquids, Solutions and Vapours, 2010, pp. 436–456, http://dx.doi.org/10.1039/9781847559791 (Chapter 20).
[45] D. Paschek, Journal of Chemical Physics 120 (2004) 6674–6690.
[46] M.R. Shirts, J.D. Chodera, Journal of Chemical Physics 129 (2008) 129105.
[47] S. Kumar, D. Bouzida, R.H. Swendsen, P.A. Kollman, J.M. Rosenberg, Journal of Computational Chemistry 13 (1992) 1011–1021.
[48] A. Pohorille, C. Jarzynski, C. Chipot, Journal of Physical Chemistry B 114 (2010) 10235–10253.